ZANCO Journal of Pure and Applied Sciences

TYPE Original article
DOI http://dx.doi.org/10.21271/ZJPAS.37.6.4

Hopf Bifurcation Analysis of the Halvorsen System

Kardo Baiz Othman[1,*] , Adnan Ali Jalal[2]

[1] Department of Physics, College of Educations-Shaqlawa, Salahaddin University-Erbil, Erbil, Iraq.

[2] Department of Mathematics, College of Education, Salahaddin University-Erbil, Erbil, Iraq.

OPEN ACCESS

*Corresponding author

Kardo Baiz Othman

kardo.othman@su.edu.krd

RECEIVED :01 /05 /2025
ACCEPTED :04/08/ 2025
PUBLISHED :31/ 12/ 2025

KEYWORDS:

Halvorsen system,
Hopf Bifurcation,
Transcritical bifurcation,
Periodic orbits,
Normal form theory.

ABSTRACT

This paper investigates local bifurcations in the Halvorsen system, focusing specifically on transcritical and Hopf bifurcations. The behavior of equilibrium points during bifurcations is studied using Sotomayor's theorem for transcritical bifurcation and normal form theory, which is based on Hassard's formulas, for Hopf bifurcation. When the bifurcation parameter exceeds a critical value, a Hopf bifurcation emerges. By applying normal form theory, we establish the conditions under which a Hopf bifurcation occurs. Furthermore, we discuss the direction of the Hopf bifurcation and the stability of the resulting periodic orbits. Finally, numerical simulations are provided to support the theoretical findings.

1.Introduction

Advancements in nonlinear dynamics have led to extensive studies incorporating bifurcation and chaos theory to better understand the behavior of dynamical systems. Since Edward Lorenz first identified chaotic behavior in 1963 (Lorenz, 1963), numerous chaotic systems have been proposed and explored, including the (Rössler, 1976), Lü system (Lü and Chen, 2002), Chen-Lee system (Chen et al., 2004), Zhou system (Zhou et al., 2008), Zhu system (Zhu et al., 2010), and Wei-Yang system (Wei and Yang, 2010). Among these, three-dimensional systems such as the Rössler, Lorenz, and Halvorsen systems are widely used to evaluate various modeling techniques. The Rössler system, though simple, provides a representative example of chaotic dynamics and is often used as a benchmark. The Lorenz system is arguably the most well-known chaotic model. In contrast, the Halvorsen system, known for its cyclic symmetry, generates rich and complex trajectories, making it ideal for analyzing systems of moderate complexity. The general form of the Halvorsen system can be written as:

$$\dot{x} = f(x,y,z),\ \dot{y} = f(y,z,x),\ \dot{z} = f(z,y,x),$$

where the function f is identical in structure but cyclically permutes its variables. One particular version of this system, as presented by Sprott (Sprott, 2010) and Thomas's system (Thomas, 1999).

According to Sprott (2003), Halvorsen's chaotic circulating system (Sprott, 2003), is achieved by taking

$$f(x,y,z) = -ax - by - bz - y^2.$$

Thus, Halvorsen's circulant chaotic system, written in its most general form (Sprott, 2023) is given by

$$\begin{aligned} \dot{x} &= f(x,y,z) = -a\,x - b\,y - c\,z - d\,y^2, \\ \dot{y} &= f(y,z,x) = -a\,y - b\,z - c\,x - d\,z^2, \\ \dot{z} &= f(z,x,y) = -a\,z - b\,x - c\,y - d\,x^2, \end{aligned} \quad (1)$$

where x, y and z are state variables and $a, b, c, d \in R$ are system parameters. Although originally proposed by Arne Dehli Halvorsen, to the best of our knowledge, no experimental validation of the Halvorsen attractor has been published. This system appears to be the most basic example, including a singular quadratic nonlinearity. System (1) includes four parameters that are repeated in the equations to preserve the requisite symmetry. In addition, system (1) has a chaotic attractor when fixed parameters and with initial condition [-5,0,0], as shown in Figure 1 (Sprott, 2003). System (1) has a conservative variant (a = 0), but only the dissipative case (a > 0) is considered here (Sprott, 2023).

The Halvorsen system has attracted significant interest in recent years. For instance, Vaidyanathan and Pakiriswamy in (Vaidyanathan and Pakiriswamy, 2014) explored generalized projective synchronization (GPS) using adaptive control and Lyapunov stability theory. In later work, Vaidyanathan and Azar in (Vaidyanathan and Azar, 2016) designed adaptive controllers and synchronizers for the Halvorsen system. Tutueva et al. (Tutueva et al., 2019) proposed a fixed-point implementation to extrapolate its dynamics. Hammouch et al. (Hammouch et al., 2021) applied a novel numerical method involving fractional differential equations with variable order. Ma et al. (Ma et al., 2022) used causal inference and Fourier transform surrogates to analyze nonlinear dependencies in the system. In (Yousfi et al., 2024), it is introduced a linear control strategy for synchronizing fractional-order Halvorsen systems using the Adomian Decomposition Method. Meanwhile, (Colak et al., 2024) analyzed a microwave absorber inspired by Halvorsen dynamics to enhance stealth technology in fighter jets. There have been some detailed investigations of Halvorsen's system in references (Miao et al., 2024, Herteux and Räth, 2020, Berir, 2024, Feng et al., 2025, Gotthans and Petrzela, 2011, Yousfi et al., 2024, Petržela et al., 2011). However, it is important to note that, based on currently available knowledge, the Hopf bifurcation of the Halvorsen system has received relatively less attention. In addition, none of these studies is specifically dedicated to providing a detailed analysis of the Hopf bifurcation using normal form theory.

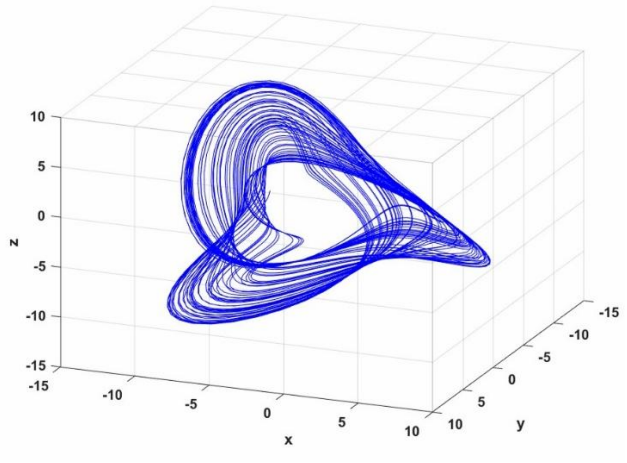

Figure 1. Phase portraits of system (1) when $a = 1.27, b = c = 4$ and $d = 1$.

Bifurcation phenomena occur when a small change in parameter values causes a sudden qualitative or topological change in behavior. Various bifurcations have been studied extensively with the three-dimensional differential system, such as Hopf bifurcation, zero-Hopf bifurcation, pitchfork bifurcation, transcritical bifurcation, saddle-node bifurcation, etc. Although significant work has focused on Hopf bifurcations, particularly their existence, direction, and the stability of bifurcating periodic orbits, this area continues to present rich opportunities for further investigation (Salih and Mohhamad, 2024, Husien and Amen, 2024). Hopf bifurcation is a type of local bifurcation that occurs in a three-dimensional system when a complex conjugate pair of linearized flow eigenvalues at an equilibrium point becomes purely imaginary and non-zero real parts. Furthermore, bifurcation requires the satisfaction of specific transversality conditions (Kuznetsov et al., 1998, Lynch, 2004). Hopf bifurcations are commonly observed in nonlinear systems and are associated with the emergence or disappearance of limit cycles around equilibrium points. Depending on the system's dynamics, the bifurcation can give rise to either a stable or unstable periodic orbit, following the destabilization of the equilibrium. In contrast, a transcritical bifurcation occurs when two equilibrium points exchange stability as a system parameter varies. This bifurcation type is characterized by the presence of a zero eigenvalue in the Jacobian matrix, with the remaining eigenvalues having negative real parts (Strogatz, 2024).

The remainder of this paper is organized as follows: Section 2 examines the stability of the system's equilibrium points using characteristic equations. Section 3 investigates the occurrence of transcritical bifurcation at the equilibrium points. Section 4 explores the conditions for the occurrence of Hopf bifurcation, including the direction and stability of the resulting periodic orbits, through the application of normal form theory. Section 5 presents numerical simulations to validate and illustrate the theoretical results. Finally, section 6 summarizes the main results derived in this paper.

2. Stability Analysis of Equilibrium Points

In this section, the stability of equilibrium points of the Halvorsen system (1) is studied. It is easy to discover that the Halvorsen system (1) has two real equilibrium points, which are $E_0(0,0,0)$ and $E_1(\eta^*, \eta^*, \eta^*)$ where $\eta^* = -\frac{a+b+c}{d}$, $d \neq 0$.

The stability properties of the equilibrium points E_0 and E_1 are rigorously characterized by the following proposition. The conditions under which each equilibrium point remains asymptotically stable or becomes unstable as the system parameters vary are specified.

Proposition 1. The stability of the equilibrium points E_0 and E_1 of system (1) is presented as follows:

i) If the condition $a + b + c < 0$ or $-2a + b + c > 0$ holds, then the equilibrium point E_0 is unstable; it is asymptotically stable if and only if $a + b + c > 0 > -2a + b + c$.

ii) If the condition $a + b + c > 0$ or $-4a + b + c < 0$ is satisfied, then the equilibrium point E_1 is unstable; it is asymptotically stable if and only if $a + b + c < 0 < -4a + b + c$.

iii) If $a = -b - c$, the equilibrium points E_0 and E_1 coalesce at the origin, resulting in the presence of nonhyperbolic eigenvalues. Then

(1) When $b + c > 0$, the equilibrium point E_0 is unstable.

(2) When $b + c < 0$ and $d < 0$, the equilibrium point E_0 is unstable. While, when $b + c < 0 < d$, then E_0 is an asymptotically stable.

Proof. The following expression represents the

Jacobian matrix of the Halvorsen system (1)

$$\begin{pmatrix} -a & -(b+2dy) & -c \\ -c & -a & -(b+2dz) \\ -(b+2dx) & -c & -a \end{pmatrix}. \quad (2)$$

(i) The corresponding characteristic polynomial at the equilibrium point E_0 is

$$\phi_{E_0}(\lambda) = \lambda^3 + C_{11}\lambda^2 + C_{12}\lambda + C_{13}, \quad (3)$$

where $C_{11} = 3a$, $C_{12} = 3(a^2 - bc)$ and $C_{13} = a^3 + b^3 + c^3 - 3\text{abc}$.

The roots of equation (3) are given by

$$\lambda_1 = -(a+b+c),$$

$$\lambda_{2,3} = \frac{1}{2}\left(-2a + b + c \mp \sqrt{3}i(-b+c)\right).$$

It is easy to see that when $a+b+c<0$ or $-2a+b+c>0$ i.e., $\lambda_1 > 0$ or $Re\lambda_{2,3} > 0$, at least one of the eigenvalues is positive. Thus, the equilibrium point E_0 is unstable see Figure 2(a). However, when $a+b+c>0>-2a+b+c$ i.e., $\lambda_1 < 0$ and $Re\lambda_{2,3} < 0$, the real parts of all the roots of equation (3) are negative. Thus, the equilibrium point E_0 is asymptotically stable, see Figure 2(b).

(ii) In addition, let us consider the characteristic polynomial that corresponds to the equilibrium point E_1 is

$$\phi_{E_1}(\lambda) = \lambda^3 + C_{21}\lambda^2 + C_{22}\lambda + C_{23}, \quad (4)$$

where $C_{21} = 3a$, $C_{22} = 3(a^2 + 2c^2 + 2ac + bc)$ and $C_{23} = -(a+b+c)(7a^2 + b^2 + 7c^2 + 5ab + 11ac + 5bc)$ be coefficients of the $\phi_{E_1}(\lambda)$. The roots of equation (4) are given by

$$\lambda_1 = a+b+c,$$

$$\lambda_{2,3} = \frac{1}{2}\left(-4a - b - c \mp \sqrt{3}i(2a+b+3c)\right).$$

When $a+b+c>0$ or $4a+b+c<0$ i.e. *Re* $\lambda_1 > 0$ or $Re\lambda_{2,3} > 0$ at least one of the eigenvalues is positive. Consequently, the equilibrium point E_1 is unstable see Figure 2(c). However, when $a+b+c<0<-4a+b+c$ i.e., $\lambda_1 < 0$ and $Re\lambda_{2,3} < 0$, the real parts of all the roots of equation (4) are negative. Hence, the equilibrium point E_1 is asymptotically stable, see Figure 2(d).

iii) Since $a = -b - c$, so the roots of equations (3) and (4) yield the following eigenvalues

$$\lambda_1 = 0 \text{ and } \lambda_{2,3} = \frac{3}{2}(b+c) \mp \frac{\sqrt{3}i}{2}(b-c).$$

Consequently, when $(b+c)>0$, the real eigenvalues $Re\lambda_{2,3}$ are positive, implying that the equilibrium point E_0 is unstable see Figure 2(e). Also, when $(b+c)<0$ the real eigenvalues $Re\lambda_{2,3}$ are negative. Therefore, the stability characteristics of the equilibrium point are due to the reduced dynamics restricted to the center manifold (Perko, 2013).

The eigenvectors of system (1) following the transformation:

$$\begin{pmatrix} x \\ y \\ z \end{pmatrix} = \begin{pmatrix} 1 & \frac{b-c+\sqrt{3}i(b+c)}{b+2c-\sqrt{3}ib} & \frac{-b+c+\sqrt{3}i(b+c)}{2b+c-\sqrt{3}ic} \\ 1 & \frac{2b+c+\sqrt{3}ic}{-b-2c+\sqrt{3}ib} & 1 \\ 1 & 1 & \frac{b+2c+\sqrt{3}ib}{-2b-c+\sqrt{3}ic} \end{pmatrix} \begin{pmatrix} u \\ v \\ w \end{pmatrix}.$$

Then, system (1) becomes

$$\begin{pmatrix} \dot{u} \\ \dot{v} \\ \dot{w} \end{pmatrix} = \begin{pmatrix} 0 & 0 & 0 \\ 0 & \frac{3}{2}(b+c) - \frac{\sqrt{3}i}{2}(b-c) & 0 \\ 0 & 0 & \frac{3}{2}(b+c) + \frac{\sqrt{3}i}{2}(b-c) \end{pmatrix} \begin{pmatrix} u \\ v \\ w \end{pmatrix} + \begin{pmatrix} \varphi_1 \\ \varphi_2 \\ \varphi_3 \end{pmatrix}, \quad (5)$$

where

$$\varphi_1 = \left(1+\sqrt{3}i\right)d\, vw - du^2,$$

$$\varphi_2 = \left(1-\sqrt{3}i\right)d\, uv + \frac{(1+\sqrt{3}i)}{2}d\, w^2,$$

$$\varphi_3 = duw - dv^2 + \sqrt{3}id\, uw.$$

Hence, represents the one-dimensional dynamics in the variable u, which can be described within the framework of the local center manifold theory of system (5) as follows:

$W^c_{loc} = \{(u,v,w) \in R^3 \mid v = h_1(u), w = h_2(u), |u| \ll 1, \text{with } \mathrm{h}_1(0) = D\mathrm{h}_1(0) = \mathrm{h}_2(0) = D\mathrm{h}_2(0) = 0\}$.

From the Taylor expansion near the origin, $h_1(u)$ and $h_2(u)$ have the following form: $h_1(u) = \sum_{i=2}^{\infty} \alpha_i u^i$ and $h_2(u) = \sum_{i=2}^{\infty} \beta_i u^i$.

Using equation (5), we obtain

$$\alpha_i = 0 \text{ and } \beta_i = 0 \text{ for all } i \geq 2,$$

and the reduced equation on W^c_{loc} to the center manifold, given by

$$\dot{u} = -du^2.$$

When $b+c<0<d$, then, $u=0$ is asymptotically stable, see Figure 2 (f). Also, when $b+c<0$ and $d<0$, then $u=0$ is unstable, see Figure 2 (g). ■

A summary of the results obtained in this section is presented in Table 1.

Table 1. Local stability of equilibrium points.

Equilibrium points	Eigenvalues $\lambda_1, \lambda_2, \lambda_3$	Conditions	Stability
E_0	$Re(\lambda_1) > 0$ or $Re(\lambda_{2,3}) > 0$	$a + b + c < 0$ or $2a + b + c > 0$	unstable
	$Re(\lambda_1) < 0$ and $Re(\lambda_{2,3}) < 0$	$a + b + c > 0 > -2a + b + c$	Asymptotically stable
	$\lambda_1 = 0$ and $Re(\lambda_{2,3}) > 0$	$a = -b - c$ and $b + c > 0$	unstable
	$\lambda_1 = 0$ and $Re(\lambda_{2,3}) < 0$	$a = -b - c, b + c < 0$ and $d < 0$	unstable
	$\lambda_1 = 0$ and $Re(\lambda_{2,3}) < 0$	$a = -b - c$ and $b + c < 0 < d$	Asymptotically stable
E_1	$Re(\lambda_1) > 0$ or $Re(\lambda_{2,3}) > 0$	$a + b + c > 0$ or $-4a + b + c < 0$	unstable
	$Re(\lambda_1) < 0$ and $Re(\lambda_{2,3}) < 0$	$a + b + c < 0 < -4a + b + c.$	Asymptotically stable

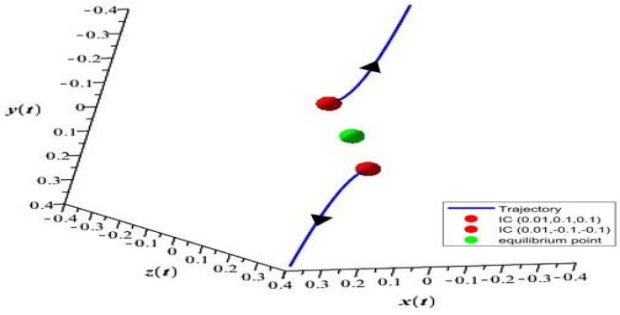

(a)

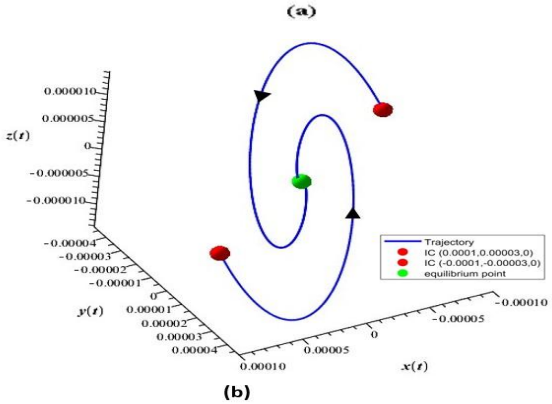

(b)

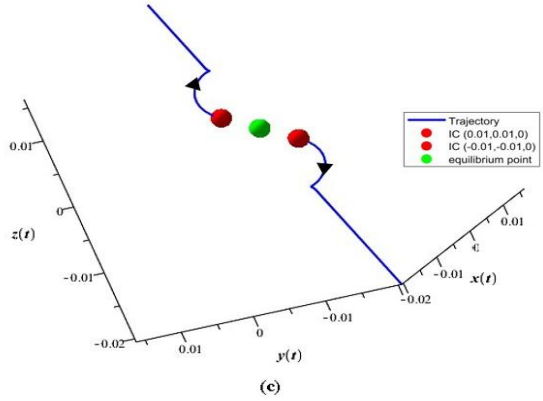

(c)

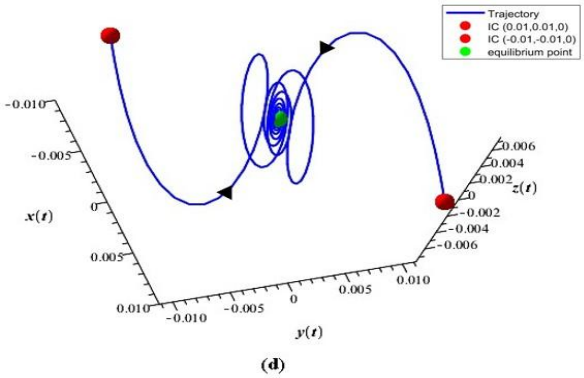

(d)

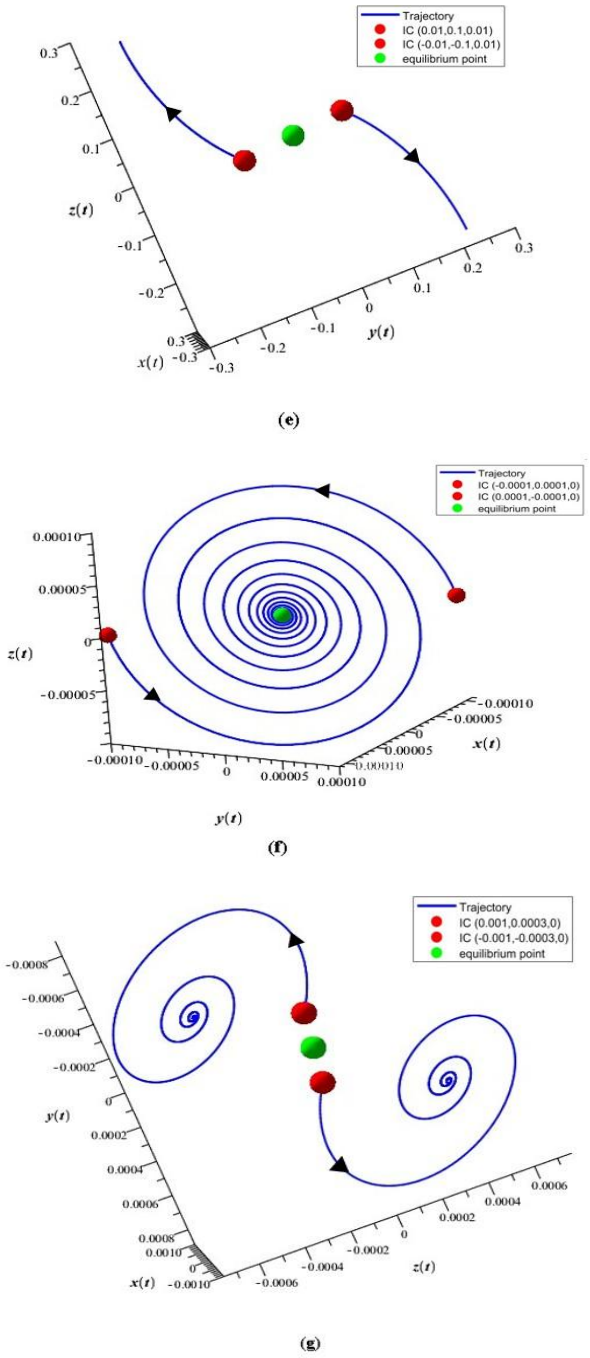

Figure 2. The phase portrait of system (1) (a) when $a = 1,\ b = -1,\ c = -3$ and $d = 2$, E_0 is unstable. (b) when $a = b = 0.1,\ c = -0.1$ and $d = 0.9,\ E_1$ is asymptotically stable. (c) when $a = 2.1,\ b = 1,\ c = -3$ and $d = 1,\ E_0$ is unstable. (d) when $a = 1,\ b = 0.1,\ c = -3$ and $d = 0.5$, E_1 is asymptotically stable. (e) when $a = -5,\ b = 0,\ c = -5$ and $d = -1,\ E_0$ is unstable. (f) when $a = 0.1,\ b = 0.9,\ c = -1$ and $d = 0.9$, E_0 is asymptotically stable. (g) when $a = 0.02,\ b = 0.1,\ c = -0.12$ and $d = -0.9,\ E_0$ is unstable.

3. Transcritical Bifurcation

Consider the following differential system.

$$\dot{x} = F(x, \mu), \quad \mu \in R, \tag{6}$$

where μ is a parameter and F is a differentiable function. Then, system (6) undergoes a transcritical bifurcation if it satisfies Sotomayor's theorem (Perko, 2013). There are certain conditions necessary for a transcritical bifurcation to exist, according to the theorem below.

Theorem 1. (Sotomayor's theorem) Consider system (6) and let there be an equilibrium $\Omega_0 \in R^n$ such that $F(\Omega_0, \mu) = 0$, for all μ, when $\mu = \mu_0$ the following condition satisfies:

1) the Jacobian matrix $J = DF(\Omega_0, \mu_0)$ has an eigenvalue $\lambda = 0$ with eigenvector v and J^T (Transpose of J) has an eigenvector w corresponding eigenvalue $\lambda = 0$. Furthermore, J has k eigenvalues with negative real parts, and $(n - k - 1)$ eigenvalues with positive real parts, where $0 \le k \le n - 1$.

2) $w^{\mathrm{T}} F_\mu(\Omega_0, \mu_0) = 0$,

3) $w^{\mathrm{T}}[DF_\mu(\Omega_0, \mu_0)v] \neq 0$,

4) $w^{\mathrm{T}}[D^2 F(\Omega_0, \mu_0)(v, v)] \neq 0$.

Then, system (6) exhibits a transcritical bifurcation at the point Ω_0 when μ pass through $\mu = \mu_0$.

In the following, we will investigate the analysis of the local transcritical bifurcation of system (1), which has two real equilibrium points E_0 and E_1 that collide at the origin when $a = -b - c$.

Theorem 2. Suppose that the Halvorsen system (1) with $d \neq 0$, a transcritical bifurcation occurs at the equilibrium points E_0 as the parameter a passes through $a = a^*$ when $a^* = -b - c$.

Proof. When $a = -b - c$, the Jacobian matrix (2) at E_0 of system (1) is

$$J_{E_0} = Df(0,0) = \begin{bmatrix} c+b & -b & -c \\ -c & c+b & -b \\ -b & -c & c+b \end{bmatrix}.$$

Then, the characteristic polynomial of J_{E_0} is given by

$$P(\lambda) = \lambda^2 - 3(b+c)\lambda + 3(b^2 + bc + c^2)\lambda,$$

when $P(\lambda) = 0$ has three roots that are simple eigenvalues $\lambda_1 = 0$, with the other nonzero real part eigenvalues $\lambda_{2,3} = \frac{3}{2}(b+c) \mp \frac{\sqrt{3}i}{2}(-b+c)$. Note that the corresponding eigenvalue $\lambda_1 = 0$ of

the matrix J_{E_0} has eigenvector $v = (1,1,1)^T$, and its transpose ${J_{E_0}}^T$ has the same eigenvector $w = (1,1,1)^T$.

According to Theorem 3, a straightforward calculation yields the following expressions:

$$w^{\mathrm{T}} f_a(E_0, a^*) = [w_1, w_2, w_3] \begin{bmatrix} \frac{\partial f_1}{\partial a} \\ \frac{\partial f_2}{\partial a} \\ \frac{\partial f_3}{\partial a} \end{bmatrix}_{(E_0, a^*)} = 0,$$

$$w^{\mathrm{T}}[Df_a(E_0, a^*)\, v] = [w_1, w_2, w_3] \begin{bmatrix} \frac{\partial^2 f_1}{\partial x \partial a} & \frac{\partial^2 f_1}{\partial y \partial a} & \frac{\partial^2 f_1}{\partial z \partial a} \\ \frac{\partial^2 f_2}{\partial x \partial a} & \frac{\partial^2 f_2}{\partial y \partial a} & \frac{\partial^2 f_2}{\partial z \partial a} \\ \frac{\partial^2 f_3}{\partial x \partial a} & \frac{\partial^2 f_3}{\partial y \partial a} & \frac{\partial^2 f_3}{\partial z \partial a} \end{bmatrix}_{(E_0, a^*)} \begin{bmatrix} v_1 \\ v_2 \\ v_3 \end{bmatrix}$$

$$= -3 \neq 0,$$

$$w^{\mathrm{T}}[D^2 f(E_0, a^*)(v, v)] = w^{\mathrm{T}} \begin{bmatrix} \sum_{i,j=1}^{3} \frac{\partial^2 f_1}{\partial x_i \partial x_j} v_i v_j \\ \sum_{i,j=1}^{3} \frac{\partial^2 f_2}{\partial x_i \partial x_j} v_i v_j \\ \sum_{i,j=1}^{3} \frac{\partial^2 f_3}{\partial x_i \partial x_j} v_i v_j \end{bmatrix}_{(E_0, a^*)} = -6d \neq 0.$$

Thus, all the conditions of Theorem 3 are satisfied. Consequently, system (1) displays a transcritical bifurcation at the equilibrium point E_0, when the parameter $a = -b - c$. ■

4. Hopf Bifurcation Analysis of the Halvorsen System

In this part, normal form theory is utilized to investigate Hopf bifurcation, its direction, stability, and increase (decrease) of the period of bifurcating periodic orbits of the Halvorsen system (1) (Hassard et al., 1981).

4.1 Hopf Bifurcation Conditions

Hopf bifurcation refers to the occurrence or non-occurrence of a limit cycle. Here, we perform a detailed Hopf bifurcation analysis for system (1). The occurrence of the Hopf bifurcation at the equilibrium points E_0 and E_1 of system (1) is analyzed. Furthermore, the direction and stability of the bifurcating periodic orbits, as well as the type of Hopf bifurcation occurring in the system, are determined using the normal form theory developed by Hassard (Hassard et al., 1981). For further information related to this work, see (Mirkhan and Amen, 2022, Salih and Mohhamad, 2024, Wu and Meng, 2025).

Theorem 3:

I) When $b = b_1^*, b_1^* = 2a - c$ with $a \neq 0$ and $a \neq$ c, equation (3) has two pure imaginary roots $\lambda_{1,2} = \mp i\omega;\ \omega = \sqrt{3}(a - c)$, and a nonzero real root $\lambda_3 = -3a$. Moreover, the complex roots cross the imaginary axis with non-zero speed, $\frac{dRe(\lambda(b))}{db}\Big|_{b=b_1^*} = \frac{1}{2} \neq 0$. Thus, system (1) displays a Hopf bifurcation at E_0 when $b = b_1^*$.

II) When $b = b_2^*, b_2^* = 2a - c$ with $a \neq 0$ and $a \neq$ c, equation (4) has two pure imaginary roots $\lambda_{1,2} = \mp i\omega;\ \omega = \sqrt{3}(a - c)$, and a nonzero real root $\lambda_3 = -3a$. Moreover, the complex roots cross the imaginary axis with non-zero speed, $\frac{dRe(\lambda(b))}{db}\Big|_{b=b_2^*} = -\frac{1}{2} \neq 0$. Thus, system (1) displays a Hopf bifurcation at E_1 when $b = b_2^*$.

Proof: I) Since $b = 2a - c$, then equation (3) can be expressed as

$$(\lambda + 3a)(\lambda^2 + 3a^2 + 3c^2 - 6ac) = 0. \quad (7)$$

Following this, the analysis of equation (7) reveals the presence of a pair of purely imaginary conjugate eigenvalues $\lambda_{1,2} = \mp i\omega$, when $\omega = \sqrt{3}(a - c)$, and a real root $\lambda_3 = -3a$, the first condition for the Hopf bifurcation is fulfilled.

Differentiating both sides of equation (3) concerning b, we obtain

$$\frac{d\lambda(b)}{db} = \frac{c\lambda + ac - b^2}{\lambda^2 + 2a\lambda + a^2 - bc}. \quad (8)$$

Taking the root $\lambda(b) = i\omega$, evaluating $b = b_1^*$, by substituting it into (8) and separating real and imaginary parts, we have

$$\alpha'(0) = \frac{dRe(\lambda(b))}{db}\Big|_{\lambda = i\omega,\, b = b_1^*} = \frac{1}{2} \neq 0$$

and

$$\omega'(0) = \frac{dIm(\lambda(b))}{db}\Big|_{\lambda = i\omega,\, b = b_1^*} = \frac{\sqrt{3}}{2}.$$

Noticeably, the second condition for Hopf

bifurcation is evidently satisfied. Thus, system (1) exhibits a Hopf bifurcation at E_0 when b passes through the critical value $b_1^* = 2a - c$.

II) At the equilibrium point E_1, when $b = b_2^* = -4a - c$, one has equation (4) that can be changed into equation (7). Consequently, the solution of equation (7) becomes $\lambda_{1,2} = \mp i\omega$, when $\omega = \sqrt{3}(a - c)$, and a real root $\lambda_3 = -3a$, the first condition for the Hopf bifurcation is fulfilled.

Differentiating both sides of equation (4) concerning b, we obtain

$$\frac{d\lambda(b)}{db} = -\frac{c\lambda - 4a^2 - 4c^2 - b^2 - 4ab - 7ac - 4bc}{\lambda^2 + 2a\lambda + a^2 + 2ac + bc}. \quad (9)$$

Taking the root $\lambda(b) = i\omega$ and evaluating $b = b_2^*$, by substituting it into (9), and separating the real and imaginary parts, leads to

$$\alpha'(0) = \frac{dRe(\lambda(b))}{db}\Big|_{\lambda = i\omega, b = b_2^*} = \frac{-1}{2} \neq 0$$

and

$$\omega'(0) = \frac{dIm(\lambda(b))}{db}\Big|_{\lambda = i\omega, b = b_2^*} = \frac{-\sqrt{3}}{2}.$$

Obviously, the second condition for Hopf bifurcation is evidently satisfied. Thus, system (1) undergoes a Hopf bifurcation at E_1 when b passes through the critical value $b_2^* = -4a - c$. ■

4.2 Direction and Stability of Bifurcation Periodic Orbits

Now, supercritical and subcritical bifurcation for the Halvorsen system (1) is considered. The normal form theory by Hassard (Hassard et al., 1981, Hassard and Wan, 1978) is used to study the local Hopf bifurcations and the direction, stability, and period of bifurcating periodic orbits in the dynamics of the system (1) are calculated through the outcomes of the values of μ_2, β_2 and τ_2.

Accordingly, the equilibrium point E_0, when $b = b_1^* = 2a - c$ is chosen as a representative for the subsequent discussion. We find the eigenvectors v_1, v_2 associated with eigenvalues $\lambda_1 = \sqrt{3}i(a - c)$ and $\lambda_3 = -3a$, be

$v_1 = \left(-1 + \sqrt{3}i, 2, -1 - \sqrt{3}i\right)^T$ and $v_2 = (1,1,1)^T$, respectively.

Let

$$T = (Re(v_1) \quad -Im(v_1) \quad v_2) = \begin{pmatrix} -1 & -\sqrt{3} & 1 \\ 2 & 0 & 1 \\ -1 & \sqrt{3} & 1 \end{pmatrix}$$

and $\begin{pmatrix} x \\ y \\ z \end{pmatrix} = T \begin{pmatrix} u \\ v \\ w \end{pmatrix}$.

Therefore, the differential system (1) will be expressed as a new system

$$\begin{aligned} \dot{u} &= -\sqrt{3}(a - c)v + P(u, v, w), \\ \dot{v} &= \sqrt{3}(a - c)u + Q(u, v, w), \\ \dot{w} &= -3aw + R(u, v, w), \end{aligned} \quad (10)$$

where

$$P(u, v, w) = d\left(\frac{1}{2}(u^2 - v^2) + \sqrt{3}\,uv + uw - \sqrt{3}vw\right),$$

$$Q(u, v, w) = d\left(\frac{\sqrt{3}}{2}(u^2 - v^2) - uv + \sqrt{3}\,uw + vw\right),$$

$$R(u, v, w) = -d(2u^2 + 2v^2 + w^2).$$

In the following, using formulas according to the procedures by Hassard (Hassard et al., 1981) and it is obtained

$$g_{11} = \frac{1}{4}\left(\frac{\partial^2 P}{\partial u^2} + \frac{\partial^2 P}{\partial v^2} + i\left(\frac{\partial^2 Q}{\partial u^2} + \frac{\partial^2 Q}{\partial v^2}\right)\right) = 0,$$

$$g_{02} = \frac{1}{4}\left(\frac{\partial^2 P}{\partial u^2} - \frac{\partial^2 P}{\partial v^2} - 2\frac{\partial^2 Q}{\partial u\,\partial v} + i\left(\frac{\partial^2 Q}{\partial u^2} - \frac{\partial^2 Q}{\partial v^2} + 2\frac{\partial^2 P}{\partial u\,\partial v}\right)\right) = d + \sqrt{3}id,$$

$$g_{20} = \frac{1}{4}\left(\frac{\partial^2 P}{\partial u^2} - \frac{\partial^2 P}{\partial v^2} + 2\frac{\partial^2 Q}{\partial u\,\partial v} + i\left(\frac{\partial^2 Q}{\partial u^2} - \frac{\partial^2 Q}{\partial v^2} - 2\frac{\partial^2 P}{\partial u\,\partial v}\right)\right) = 0,$$

$$G_{21} = \frac{1}{4}\left(\frac{\partial^3 P}{\partial u^3} + \frac{\partial^3 P}{\partial u\,\partial v^2} + \frac{\partial^3 Q}{\partial u^2 \partial v} + \frac{\partial^3 Q}{\partial v^3} + i\left(\frac{\partial^3 Q}{\partial u^3} + \frac{\partial^3 Q}{\partial u\,\partial v^2} - \frac{\partial^3 P}{\partial u^2 \partial v} - \frac{\partial^3 P}{\partial v^3}\right)\right) = 0.$$

Next, we calculate

$$h_{11} = \frac{1}{4}\left(\frac{\partial^2 R}{\partial u^2} + \frac{\partial^2 R}{\partial v^2}\right) = -2d,$$

$$h_{20} = \frac{1}{4}\left(\frac{\partial^2 R}{\partial u^2} - \frac{\partial^2 R}{\partial v^2} - 2\,i\,\frac{\partial^2 R}{\partial u\,\partial v}\right) = 0.$$

By solving the following equations

$$\lambda_3\,\psi_{11} = -h_{11},$$
$$(\lambda_3 - 2\,i\,\omega)\,\psi_{20} = -h_{20},$$

the solution ψ_{11} and ψ_{20} is

$$\psi_{11} = -\frac{2}{3}\frac{d}{a},$$
$$\psi_{20} = 0.$$

Furthermore, we have

$G_{110} = \frac{1}{2}\left(\frac{\partial^2 P}{\partial u\,\partial w} + \frac{\partial^2 Q}{\partial v\,\partial w} + i\left(\frac{\partial^2 Q}{\partial u\,\partial w} - \frac{\partial^2 P}{\partial v\,\partial w}\right)\right) = d + \sqrt{3}id,$

$G_{101} = \frac{1}{2}\left(\frac{\partial^2 P}{\partial u\,\partial w} - \frac{\partial^2 Q}{\partial v\,\partial w} + i\left(\frac{\partial^2 Q}{\partial u\,\partial w} + \frac{\partial^2 P}{\partial v\,\partial w}\right)\right) = 0,$

$g_{21} = G_{21} + 2\,G_{110}\psi_{11} + G_{101}\psi_{20} = -\frac{4}{3}\frac{d^2}{a} - \frac{4}{\sqrt{3}}i\frac{d^2}{a}.$

As a result of the above analysis, the following quantities can be calculated:

$\Phi_1(0) = \frac{i}{2\omega}\left(g_{20}g_{11} - \frac{1}{3}|g_{02}|^2 - 2|g_{11}|^2\right) + \frac{1}{2}g_{21} = -\frac{2}{3}\frac{d^2}{a} - \frac{2i}{3\sqrt{3}}\frac{d^2(4a-3c)}{a(a-c)},$

$\mu_2 = -\frac{Re(\Phi_1(0))}{\alpha'(0)} = \frac{4}{3}\frac{d^2}{a},$

$\beta_2 = 2\,Re\left(\Phi_1(0)\right) = -\frac{4}{3}\frac{d^2}{a},$ (11)

$\tau_2 = -\frac{Im\left(\Phi_1(0)\right) + \mu_2\,\omega'(0)}{\omega(0)} = -\frac{2}{9}\frac{d^2}{(a-c)^2},$

where $\alpha'(0) = \frac{1}{2}$ and $\omega(0) = \frac{1}{2}\sqrt{3}.$

Theorem 4. The sign of μ_2, β_2 and τ_2 determines the direction of Hopf bifurcation at the equilibrium point E_0 and the conclusions are summarized as follows:

(I) When $\mu_2 > 0(\text{resp.} < 0)$, then the Hopf bifurcation is supercritical (resp. subcritical) and the bifurcating periodic orbits exist for $b > b_1^*(b < b_1^*)$.

(II) When $\beta_2 > 0(\text{resp.} < 0)$, then the stability of the bifurcating periodic orbits is unstable (resp. stable).

(III) When $\tau_2 > 0$ $(\text{resp.} < 0)$, then the period of bifurcating periodic orbits increases (resp. decreases).

We proceed by utilizing normal form theory to establish the direction of the Hopf bifurcation and to examine the stability of the limit cycles bifurcating from the equilibrium point E_1.

For the equilibrium E_1 of system (1), it needs to be translated to the origin under the following transformation $x_1 = x - \eta^*$, $y_1 = y - \eta^*$ and $z_1 = z - \eta^*$ where $\eta^* = -(a+b+c)/d$. Then, the system (1) becomes

$$\begin{aligned} \dot{x_1} &= -ax_1 + (2a+b+2c)y_1 - cz_1 - dy_1^2, \\ \dot{y_1} &= -cx_1 - ay_1 + (2a+b+2c)z_1 - dz_1^2, \\ \dot{z_1} &= (2a+b+2c)x_1 - cy_1 - az_1 - dx_1^2. \end{aligned} \quad (12)$$

It has been demonstrated that a Hopf bifurcation occurs at the point E_1 when $b = b_2^* = -4a - c$. At first, we find the eigenvectors v_1, v_2 associated with eigenvalues $\lambda_1 = \sqrt{3}i(a-c)$ and $\lambda_3 = -3a$ $v_1 = \left(-1+\sqrt{3}i, 2, -1-\sqrt{3}i\right)^T$, $v_2 = (1,1,1)^T$, respectively.

We define T as

$T = (Re(v_1) \quad -Im(v_1) \quad v_3) = \begin{pmatrix} -1 & -\sqrt{3} & 1 \\ 2 & 0 & 1 \\ -1 & \sqrt{3} & 1 \end{pmatrix}$ and $\begin{pmatrix} x_1 \\ y_1 \\ z_1 \end{pmatrix} = T\begin{pmatrix} u \\ v \\ w \end{pmatrix}.$

Therefore, the system (1) will be a new system expression that is changed to

$$\begin{aligned} \dot{u} &= -\sqrt{3}(a-c)v + P(u,v,w), \\ \dot{v} &= \sqrt{3}(a-c)u + Q(u,v,w) \\ \dot{w} &= -3aw + R(u,v,w), \end{aligned} \quad (13),$$

where

$P(u,v,w) = d\left(\frac{1}{2}(u^2 - v^2) + \sqrt{3}\,uv + uw - \sqrt{3}vw\right),$

$Q(u,v,w) = d\left(\frac{\sqrt{3}}{2}(u^2 - v^2) - uv + \sqrt{3}uw + vw\right),$

$R(u,v,w) = -d(2u^2 + 2v^2 + w^2).$

However, the derivation process of the other equilibrium point E_1 is similar and the calculations to find $g_{11}, g_{02}, g_{20}, G_{21}, h_{11}, h_{20}, \psi_{11}, \psi_{20}, G_{110}, G_{101}, g_{21}$ and $\phi_1(0)$ are not challenging. Below are some of the results produced using Maple.

$\mu_2 = -\frac{Re(\phi_1(0))}{\alpha'(0)} = -\frac{4}{3}\frac{d^2}{a},$

$\beta_2 = 2\,Re\left(\phi_1(0)\right) = -\frac{4}{3}\frac{d^2}{a},$ (14)

$\tau_2 = -\frac{Im\left(\phi_1(0)\right) + \mu_2(a,b)\omega'(0)}{\omega_0(0)} = \frac{2}{9}\frac{d^2}{(a-c)^2},$

where $\alpha'(0) = -\frac{1}{2}$ and $\omega(0) = -\frac{1}{2}\sqrt{3}.$

Theorem 5. The sign of μ_2, β_2 and τ_2 determines the direction of Hopf bifurcation at the equilibrium point E_1 and the conclusions are summarized as follows:

(I) When $\mu_2 > 0(\text{resp.} < 0)$, then the Hopf bifurcation is supercritical (resp. subcritical) and bifurcation periodic orbits exist for $b > b_2^*(b < b_2^*)$.

(II) When $\beta_2 > 0(\text{resp.} < 0)$, then the stability of the bifurcating periodic orbits is unstable (resp. stable).

(III) When $\tau_2 > 0$ $(\text{resp.} < 0)$, then the period of bifurcating periodic orbits increases (resp. decreases).

5. Numerical Examples

In this section, we present theoretical analyses for two specific cases of the Halvorsen system using initial conditions: $[x(0) = 0,\ y(0) = z(0) = 0.5]$, with step size: 0.05 for equilibrium points E_0 and E_1, respectively.

Case 1: We choose the parameters, $a = 2,\ c = 1$ and $d = 2.1$. The theoretical analysis coordinates Theorem 4. We have the Hopf bifurcation occur when the critical value $b_1^* = 3$ and $\omega = \sqrt{3}$. The following values are calculated:

$$\mu_2 = 2.94, \quad \beta_2 = -2.94 \quad \text{and} \quad \tau_2 = -0.98.$$

- Since $\mu_2 > 0$ and $\beta_2 < 0$, then the type of Hopf bifurcation is supercritical, and bifurcating periodic orbits exist for $b < b_1^*$ and stable, as shown in Figures 3 and 4.
- Since $\tau_2 < 0$, period of bifurcating periodic orbits decreases.

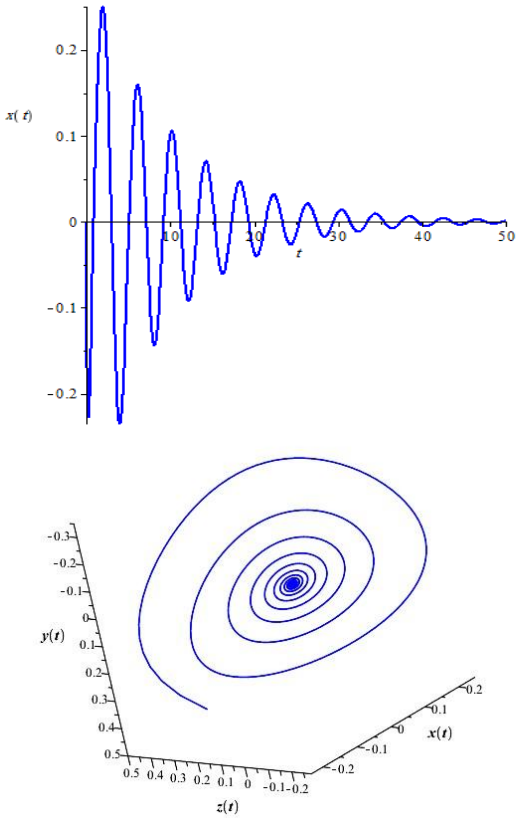

Figure 3. Time series and phase diagram for system (1) with $b = 2.8$.

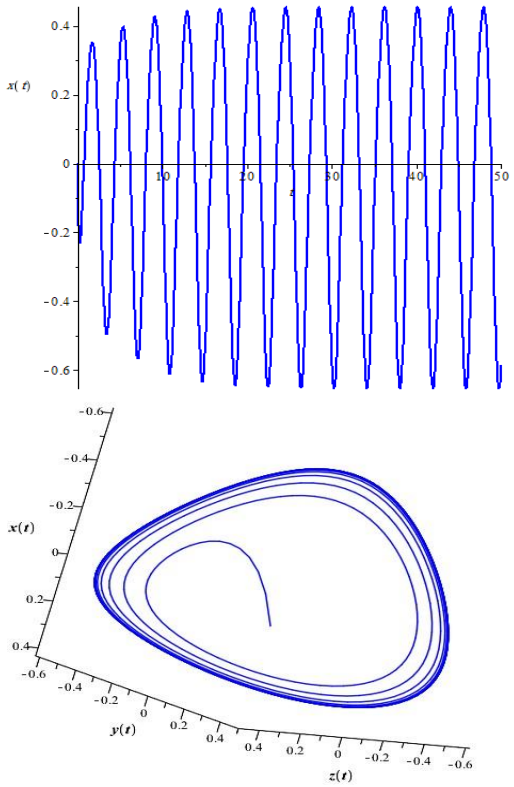

Figure 4. Time series and phase diagram for system (1) with $b = 3.2$.

Case 2: We choose the parameter $a = 1, c = -1$, and $d = 2.1$. The theoretical analysis coordinates Theorem 5. We have the Hopf bifurcation occur when the critical value $b_2^* = -3$ and $\omega = \sqrt{3}$ the following values are calculated:

$$\mu_2 = \beta_2 = -5.88 \quad \text{and} \quad \tau_2 = 0.245.$$

- Since $\mu_2 < 0$ and $\beta_2 < 0$, then the type of Hopf bifurcation is subcritical, and bifurcating periodic orbits exist for $b < b_2^*$ and stable, as shown in Figures 5 and 6.
- Since $\tau_2 > 0$, period of bifurcating periodic orbits increases.

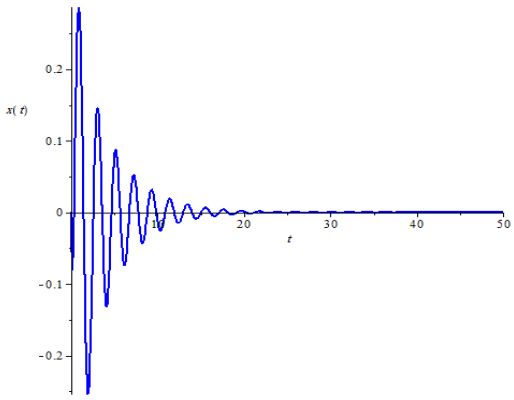

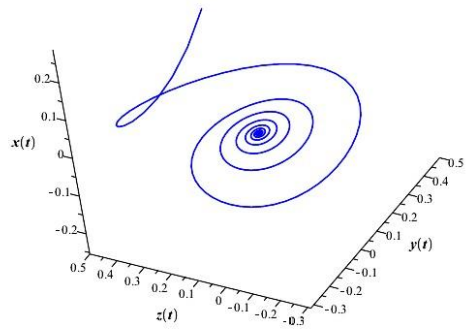

Figure 5. Time series and phase diagram for system (10) with $b = -2.5$.

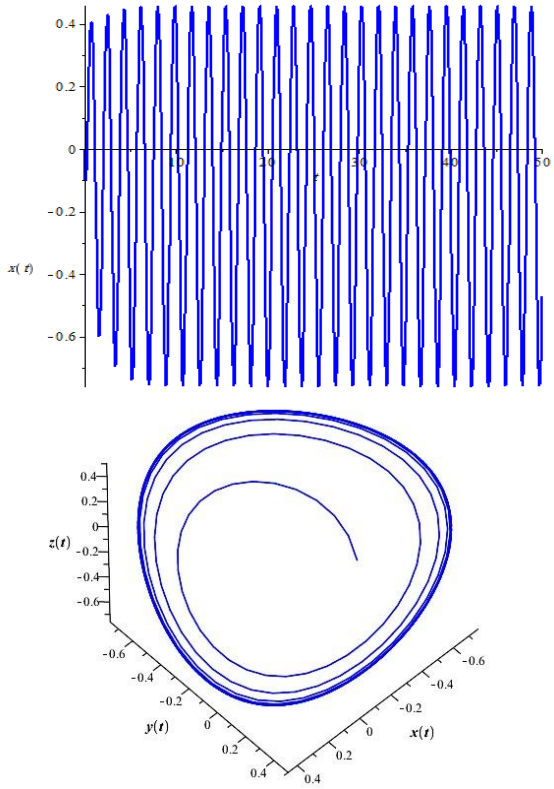

Figure 6. Time series and phase diagram for system (10) with $b = -3.5$.

6. Conclusion

In this paper, we have investigated the dynamics of the Halvorsen system (1), focusing on the stability of equilibrium points and the occurrence of local bifurcations, including transcritical and Hopf bifurcations. Firstly, the stability of the hyperbolic and non-hyperbolic equilibrium points is analyzed, see Table 1. Secondly, transcritical bifurcation is detected at the equilibrium point E_0 when the parameter a passes through $a = -b - c$. Lastly, it has been demonstrated that under certain conditions, the Hopf bifurcation occurs at the equilibrium points E_0 and E_1, as the parameter b passes through $b = 2a - c$ and $b = -4a - c$, respectively. At the equilibrium point E_1, when $a > 0$, then $\mu_2 > 0$ and $\beta_2 < 0$, the Hopf bifurcation is supercritical type and the bifurcating periodic orbits exist for $b > b_1^*$ and are stable. However, when $a < 0$, then $\mu_2 < 0$ and $\beta_2 > 0$, the Hopf bifurcation is subcritical type and the bifurcating periodic orbits exist for $b < b_1^*$ and are unstable. Since $\tau_2 < 0$, the period of bifurcating periodic orbits always decreases. At the equilibrium point E_1, when $a > 0$, then $\mu_2 > 0$ and $\beta_2 > 0$, the Hopf bifurcation is supercritical type and the bifurcating periodic orbits exist for $b > b_2^*$ and are unstable. On the contrary, when $a < 0$, then $\mu_2 < 0$ and $\beta_2 < 0$, the Hopf bifurcation is subcritical type, and the bifurcating periodic orbits exist for $b < b_2^*$ and are stable. Since $\tau_2 > 0$, the period of bifurcating periodic orbits always increases. Additionally, the stability and nature of these periodic orbits were illustrated through time series and phase diagram plots, as shown in Figures 3–6, providing visual confirmation of the theoretical results.

Acknowledgment

The authors gratefully acknowledge the support provided by Salahaddin University-Erbil, Iraq, which facilitated the execution of this study.

References

Berir, M. 2024. Analysis of the Effect of White Noise on the Halvorsen System of Variable-Order Fractional Derivatives Using a Novel Numerical Method. *International Journal of Advances in Soft Computing and its Applications,* 16**,** 294-306.

Chen, H.-K., Lee, C.-I. & Fractals. 2004. Anti-control of chaos in rigid body motion. *Chaos, Solitons,* 21**,** 957-965.

Colak, B., Karaaslan, M., Alkurt, F. O., Bakir, M., Akdogan, V., Oral, M. & Koksal, A. S. 2024. Halvorsen chaotic system based microwave absorber modelling for fighter jet stealth technologies. *Optik,* 317**,** 172075.

Feng, L., Liu, Y., Shi, B. & Liu, J. 2025. Toward a physics-guided machine learning approach for predicting chaotic systems dynamics. *Frontiers in Big Data,* 7**,** 1506443.

Gotthans, T. & Petrzela, J. 2011. Novel quantification for chaotic dynamical systems with large state attractors. *Recent Researches in Mathematical Methods in Electrical Engineering Computer Science*.

Hammouch, Z., Yavuz, M. & Özdemir, N. 2021. Numerical solutions and synchronization of a variable-order fractional chaotic system. *Mathematical Modelling and Numerical Simulation with Applications,* 1**,** 11-23.

Hassard, B. & Wan, Y. H. 1978. Bifurcation formulae derived from center manifold theory. *Journal of Mathematical Analysis Applications,* 63**,** 297-312.

Hassard, B. D., Kazarinoff, N. D. & Wan, Y.-H. 1981. *Theory and applications of Hopf bifurcation*, CUP Archive.

Herteux, J. & Räth, C. 2020. Breaking symmetries of the reservoir equations in echo state networks. *Chaos: An Interdisciplinary Journal of Nonlinear Science,* 30.

Husien, A. M. & Amen, A. I. 2024. Hopf and Zero-Hopf Bifurcation Analysis for a Chaotic System. 34**,** 2450104.

Kuznetsov, Y. A., Kuznetsov, I. A. & Kuznetsov, Y. 1998. *Elements of applied bifurcation theory*, Springer.

Lorenz, E. N. 1963. The mechanics of vacillation. *Journal of Atmospheric Sciences,* 20**,** 448-465.

Lü, J. & Chen, G. 2002. A new chaotic attractor coined. *International Journal of Bifurcation chaos,* 12**,** 659-661.

Lynch, S. 2004. *Dynamical systems with applications using MATLAB*, Springer.

Ma, H., Haluszczynski, A., Prosperino, D. & Räth, C. 2022. Identifying causality drivers and deriving governing equations of nonlinear complex systems. *Chaos: An Interdisciplinary Journal of Nonlinear Science,* 32.

Miao, H., Zhu, W., Dan, Y. & Yu, N. 2024. Chaotic time series prediction based on multi-scale attention in a multi-agent environment. *Chaos, Solitons Fractals,* 183**,** 114875.

Mirkhan, J. M. & Amen, A. I. 2022. Bifurcation analysis for Shil'nikov Chaos Electro-dissolution of Copper. *Zanco Journal of Pure and Applied Sciences,* 34**,** 83-91.

Perko, L. 2013. *Differential equations and dynamical systems*, Springer Science & Business Media.

Petržela, J., Hruboš, Z. & Gotthans, T. 2011. Modeling Deterministic Chaos Using Electronic Circuits. *Radioengineering,* 20.

Rössler, O. E. 1976. An equation for continuous chaos. *Physics Letters A,* 57**,** 397-398.

Salih, H. R. & Mohhamad, B. 2024. Stability and Hopf bifurcation in a modified Sprott C system. *Tatra Mt. Math. Publ,* 88**,** 59-72.

Sprott, J. 2003. Chaos and Time-Series Analysis. Oxford University Press.

Sprott, J. C. 2010. *Elegant chaos: algebraically simple chaotic flows*, World Scientific.

Sprott, J. C. 2023. *Elegant Automation: Robotic Analysis of Chaotic Systems*, World Scientific.

Strogatz, S. H. 2024. *Nonlinear dynamics and chaos: with applications to physics, biology, chemistry, and engineering*, Chapman and Hall/CRC.

Thomas, R. 1999. Deterministic chaos seen in terms of feedback circuits: Analysis, synthesis," labyrinth chaos". *International Journal of Bifurcation and Chaos,* 9**,** 1889-1905.

Tutueva, A., Andreev, V., Karimov, T., Kopets, E. & Khalyasmaa, A. Fixed-Point Implementation of Extrapolation ODE Solvers. 2019 Ural Symposium on Biomedical Engineering, Radioelectronics and Information Technology (USBEREIT), 2019. IEEE, 310-312.

Vaidyanathan, S. & Azar, A. T. 2016. Adaptive control and synchronization of Halvorsen circulant chaotic systems. *Advances in chaos theory and intelligent control.* Springer.

Vaidyanathan, S. & Pakiriswamy, S. 2014. Adaptive Controller Design for the Generalized Projective Synchronization of Circulant Chaotic Systems with Unknown Parameters. *International Journal of Control Theory and Applications,* 7**,** 55-74.

Wei, Z. & Yang, Q. 2010. Anti-control of Hopf bifurcation in the new chaotic system with two stable node-foci. *Applied Mathematics Computation,* 217**,** 422-429.

Wu, S.-X. & Meng, X.-Y. 2025. Hopf bifurcation analysis of a multiple delays stage-structure predator-prey model with refuge and cooperation. *Electronic Research Archive,* 33.

Yousfi, H., Islam, Y., He, S., Gasri, A. & Hassan, M. M. 2024. Advanced medical image encryption techniques using the fractional-order Halvorsen circulant systems: dynamics, control, synchronization and security applications. *Physica Scripta,* 99**,** 055208.

Zhou, W., Xu, Y., Lu, H. & Pan, L. 2008. On dynamics analysis of a new chaotic attractor. *J Physics Letters A,* 372**,** 5773-5777.

Zhu, C., Liu, Y. & Guo, Y. 2010. Theoretic and numerical study of a new chaotic system. *J Intelligent Information Management,* 2**,** 104-109.